

[Article]

www.whxb.pku.edu.cn

## N(<sup>4</sup>S)+NO(X<sup>2</sup>II)→N<sub>2</sub>(X<sup>3</sup>Σ<sub>g</sub><sup>-</sup>)+O(<sup>3</sup>P)反应的立体动力学

马建军 张志红 丛书林\*

(大连理工大学物理系, 辽宁 大连 116024)

**摘要** 采用准经典轨线方法研究了在不同碰撞能下, 碰撞反应 N(<sup>4</sup>S)+NO(X<sup>2</sup>II)→N<sub>2</sub>(X<sup>3</sup>Σ<sub>g</sub><sup>-</sup>)+O(<sup>3</sup>P)在两个最低势能面 <sup>3</sup>A''和 <sup>3</sup>A'产物与反应物之间的矢量相关. 结果表明, 对于不同的碰撞能, 在两个势能面上反应产物的转动取向展示了不同的特征和趋势. 发生在 <sup>3</sup>A''势能面上的反应主要由外平面机理支配, 而发生在 <sup>3</sup>A'势能面上的反应倾向于受内平面机理支配. 这些差异来自于两个势能面的不同构型.

**关键词:** 准经典轨线, 矢量相关, 立体动力学, 取向与定向, 碰撞反应

**中图分类号:** O641.6

## Stereodynamics Study of N(<sup>4</sup>S)+NO(X<sup>2</sup>II)→N<sub>2</sub>(X<sup>3</sup>Σ<sub>g</sub><sup>-</sup>)+O(<sup>3</sup>P) Reaction

MA, Jian-Jun ZHANG, Zhi-Hong CONG, Shu-Lin\*

(Department of Physics, Dalian University of Technology, Dalian 116024, P. R. China)

**Abstract** The vector correlations between products and reagents for the reaction N(<sup>4</sup>S)+NO(X<sup>2</sup>II)→N<sub>2</sub>(X<sup>3</sup>Σ<sub>g</sub><sup>-</sup>)+O(<sup>3</sup>P) are studied by using quasiclassical trajectory (QCT) method at different collision energies on two lowest <sup>3</sup>A'' and <sup>3</sup>A' potential energy surfaces (PESs). The results indicate that the product rotational polarizations on the two PESs exhibit different characters and trends at different collision energies. The rotational angular momentum *j'* of the product molecule N<sub>2</sub> is not only aligned, but also is oriented on both PESs. The reaction occurred on the <sup>3</sup>A'' PES is mainly dominated by out-of-plane mechanism, while that occurred on the <sup>3</sup>A' PES tends to be dominated by in-plane mechanism. All these differences arise from different configurations of the two PESs.

**Keywords:** Quasiclassical trajectory, Vector correlations, Stereodynamics, Alignment and orientation, Collision reaction

The gas-phase reaction N(<sup>4</sup>S)+NO(X<sup>2</sup>II)→N<sub>2</sub>(X<sup>3</sup>Σ<sub>g</sub><sup>-</sup>)+O(<sup>3</sup>P) and its reverse reaction play a crucial role in the Earth's atmospheric chemistry<sup>[1-4]</sup>. To date, the theoretical<sup>[5-9]</sup> and experimental<sup>[10-11]</sup> studies about this reaction mainly involve its scalar properties, such as the rate constant, the reaction cross-sections, and the internal energy distribution of products. This reaction can proceed on the ground state <sup>3</sup>A'' and the first excited state <sup>3</sup>A' potential energy surfaces (PESs). Besides, there also exists the second reaction channel: N(<sup>4</sup>S)+NO(X<sup>2</sup>II)→NO(X<sup>2</sup>II)+N(<sup>3</sup>P), which only occurs at higher collision energies (*E*<sub>T</sub> > 1.3 eV). Recently,

Sayós *et al.*<sup>[8]</sup> described the character of stationary points of the lowest <sup>3</sup>A'' and <sup>3</sup>A' PESs and confirmed that the <sup>3</sup>A'' PES has no energy barrier and the <sup>3</sup>A' PES has an energy barrier of about 0.3 eV for the first reaction channel. Based on the *ab initio* data, they presented new analytical <sup>3</sup>A'' and <sup>3</sup>A' PESs<sup>[9]</sup>. The new analytical PESs may provide better dynamical information about this reaction.

The vector property of chemical reaction can provide valuable information about chemical reactive stereodynamics<sup>[12-15]</sup>. Many experimental techniques, such as polarization-resolved

Received: January 27, 2006; Revised: March 25, 2006. \*Correspondent, E-mail: shlcong@dlut.edu.cn; Tel: 0411-84706121.

国家自然科学基金(10374012)资助项目

chemiluminescence and polarized laser-induced fluorescence, have been used to measure the vector correlations between the reagents and products<sup>[16-18]</sup>. Theoretically, the quasiclassical trajectory (QCT), quantum-scattering, and wave packet dynamics methods have been employed to describe the angular momentum polarizations of product and the vector correlations between the reagents and products<sup>[19,26]</sup>. In the present work, the reaction dynamics of the first reaction channel has been studied because of its importance. The attention focused on stereodynamics characters of the title reaction based on the  $^3A''$  and  $^3A'$  PESs given by Sayós *et al.*<sup>[9]</sup>.

## 1 Computational method

The general theory of the QCT method can be found in literatures [27-31]. Only the details relevant to the present work are summarized here. The reference frame is shown in Fig.1. The  $z$ -axis is parallel to initial relative velocity vector  $\mathbf{k}$  and  $x$ - $z$  is the scattering plane containing the initial and final relative velocity vectors,  $\mathbf{k}$  and  $\mathbf{k}'$ . And the  $y$ -axis is perpendicular to the  $x$ - $z$  plane.  $\theta_i$  is the scattering angle (i.e. the angle between  $\mathbf{k}$  and  $\mathbf{k}'$ ),  $\theta_r$  and  $\phi_r$  are the polar and azimuthal angle of the final rotational angular momentum  $\mathbf{j}'$ , and  $\theta_{tr}$  denotes the angle between  $\mathbf{k}'$  and  $\mathbf{j}'$ .

The distribution function  $P(\theta_r)$  describing the  $\mathbf{k}$ - $\mathbf{j}'$  correlation can be expanded in a series of Legendre polynomials as<sup>[31]</sup>

$$P(\theta_r) = \frac{1}{2} \sum_k (2k+1) a_0^{(k)} P_k(\cos\theta_r) \quad (1)$$

with

$$a_0^{(k)} = \int_0^\pi P(\theta_r) P_k(\cos\theta_r) \sin\theta_r d\theta_r = \langle P_k(\cos\theta_r) \rangle \quad (2)$$

The expanding coefficients  $a_0^{(k)}$  or  $\langle P_k(\cos\theta_r) \rangle$  are called orientation ( $k$  is odd) and alignment ( $k$  is even) parameters. In the computation, the  $P(\theta_r)$  is expanded up to  $k=18$ , which shows a good convergence.

The dihedral angle distribution function  $P(\phi_r)$  describing  $\mathbf{k}$ - $\mathbf{k}'$ - $\mathbf{j}'$  correlation can be expanded in Fourier series as

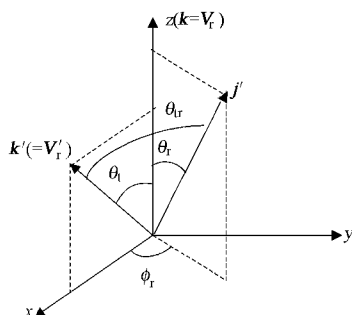


**Fig.1** The center of mass coordinate system used to describing the  $\mathbf{k}$ ,  $\mathbf{k}'$ , and  $\mathbf{j}'$  correlations

$$P(\phi_r) = \frac{1}{2\pi} \left( 1 + \sum_{\text{even } n \geq 2} a_n \cos n\phi_r + \sum_{\text{odd } n \geq 1} b_n \sin n\phi_r \right) \quad (3)$$

where

$$a_n = 2 \langle \cos n\phi_r \rangle \quad (4)$$

$$b_n = 2 \langle \sin n\phi_r \rangle \quad (5)$$

In the calculation,  $P(\phi_r)$  is expanded up to  $n=24$  with a good convergence.

The vector correlation between the reagent and product can be expressed as<sup>[31]</sup>

$$P(\omega_r, \omega_r) = \sum_{kq} \frac{2k+1}{4\pi} P_{kq}(\omega_r) C_{kq}(\theta_r, \phi_r)^* \quad (6)$$

where  $C_{kq}(\theta_r, \phi_r) = \sqrt{4\pi/(2k+1)} Y_{kq}(\theta_r, \phi_r)$  is the modified spherical harmonics,  $P_{kq}(\omega_r)$  denotes a generalized polarization-dependent differential cross section (PDDCS), which is defined as

$$P_{kq}(\omega_r) = \frac{1}{\sigma} \frac{d\sigma_{kq}}{d\omega_r} = \int P(\omega_r, \omega_r) C_{kq}(\theta_r, \phi_r) d\omega_r \quad (7)$$

where  $d\omega_r = \sin\theta_r d\theta_r d\phi_r$ . When  $q \neq 0$ ,  $P_{kq}(\omega_r)$  are complex spherical tensor operators. For convenience, using the formulas of Hertel and Stoll<sup>[32]</sup>, one can convert the complex quantities into real ones. The real  $P_{kq}(\omega_r)$  with  $q \neq 0$  are defined as<sup>[30, 32-33]</sup>

$$\begin{aligned} P_{kq\pm}(\omega_r) &= \frac{1}{\sqrt{2}} i^{(-1\pm 1)} [P_{kq}(\omega_r) \pm P_{k-q}(\omega_r)] \\ &= \frac{1}{\sqrt{2}} i^{(-1\pm 1)} (-1)^q [1 \pm (-1)^k] \sum_{k_1 \geq q} \frac{2k+1}{4\pi} s_{k_1 q}^k C_{k_1 q}(\theta_r, 0) \end{aligned} \quad (8)$$

with

$$s_{k_1 q}^k = (-1)^q \langle C_{k_1 q}(\theta_r, 0) C_{kq}(\theta_r, 0) \exp(iq\phi_r) \rangle \quad (9)$$

where the brackets indicate averaging over all the trajectories. When  $k$  is even and  $q=0$ ,  $P_{kq}(\omega_r)$  reduces to

$$P_{k0}(\omega_r) = \frac{1}{4\pi} \sum_{k_1} (2k_1+1) s_{k_1 0}^k P_{k_1}(\cos\theta_r) \quad (10)$$

with

$$s_{k_1 0}^k = 2\pi \int_{-1}^1 P_{k_1}(\omega_r) P_k(\cos\theta_r) d(\cos\theta_r) = \langle P_{k_1}(\cos\theta_r) \cdot P_k(\cos\theta_r) \rangle \quad (11)$$

A renormalized PDDCS is given by

$$\tilde{P}_{kq\pm}(\omega_r) = P_{kq\pm}(\omega_r) / P_{00}(\omega_r) \quad (12)$$

The calculating method of QCT is the same as that of literatures [27-31]. The classical Hamilton's equations are numerically integrated in three dimensions. Due to the different energy barriers on the two PESs, collision energies ( $E_r$ ) were chosen as 0.0388, 0.6, and 1.0 eV for the  $^3A''$  PES and 0.6, 1.0, and 1.8 eV for the  $^3A'$  PES, respectively. The accuracy of the numerical integration is verified by checking the conservation of the total energy and total angular momentum for every trajectory. The vibrational and rotational levels of NO molecule are taken as  $\nu=0$  and  $j=7$ . In the calculation, batches of 500000 trajectories are run for each collision energy and the integration step is chosen as 0.05 fs. The trajectories are started at an initial distance of 1.0 nm be-

tween the N( $^4S$ ) atom and the center of mass of the NO molecule.

## 2 Results and discussion

The calculated distributions of  $P(\theta_r)$  and  $P(\phi_r)$  on the  $^3A''$  PES for three collision energies (0.0388, 0.6, and 1.0 eV) are shown in Fig.2(a) and Fig.2(b), respectively. The distributions of  $P(\theta_r)$  display a peak at  $\theta_r=90^\circ$  and are symmetry with respect to  $90^\circ$ , which means that the product rotational angular momentum vector  $\mathbf{j}'$  is strongly aligned along the direction perpendicular to the relative velocity vector. The peak of  $P(\theta_r)$  becomes thinner and higher with the collision energy increasing, indicating that higher collision energy will cause strong alignment of the product N<sub>2</sub>. The dihedral angle distributions  $P(\phi_r)$  are shown in Fig.2(b). The distributions of  $P(\phi_r)$  are asymmetric with respect to the  $\mathbf{k-k}'$  scattering plane (or about  $\phi_r=180^\circ$ ). The peaks of  $P(\phi_r)$  appear at  $\phi_r=90^\circ$  and  $270^\circ$ , which shows that the angular momentum  $\mathbf{j}'$  of the product N<sub>2</sub> is aligned along y-axis of the frame. The peaks at  $\phi_r=90^\circ$  are not equal to those at  $\phi_r=270^\circ$ , meaning that the angular momentum  $\mathbf{j}'$  is not only aligned, but also oriented along the y-axis. The orientation of angular momentum  $\mathbf{j}'$  depends sensitively on the collision energy  $E_T$ . When the collision energy increases, the angular momentum  $\mathbf{j}'$  tends to be

strongly oriented along the negative direction of y-axis. The broader distribution at  $\phi_r=270^\circ$  for higher collision energy indicates that the reaction is mainly dominated by out-of-plane mechanism, in which the product molecule prefers rotating in a plane perpendicular to the scattering plane<sup>[25]</sup>.

The distributions of  $P(\theta_r)$  and  $P(\phi_r)$  on the  $^3A'$  PES are shown in Fig.3. The distributions of  $P(\theta_r)$  and  $P(\phi_r)$  on the  $^3A'$  PES differ from those on the  $^3A''$  PES. When the collision energy increases, the peak at  $\theta_r=90^\circ$  becomes broader and lower, indicating that the alignment effect of the product becomes weak. The distributions of  $P(\phi_r)$  are asymmetric with respect to the  $\mathbf{k-k}'$  scattering plane. The peaks of distributions at  $\phi_r=270^\circ$  are stronger than those at  $\phi_r=90^\circ$ , indicating that the  $\mathbf{j}'$  is preferentially oriented along the negative direction of y-axis. However, the peaks at  $\phi_r=270^\circ$  become thinner and higher with the increase of the collision energy, meaning that the reaction is mainly dominated by in-plane mechanism, in which the product molecule prefers rotating in the scattering plane<sup>[25]</sup>.

The difference between the rotational polarizations of product N<sub>2</sub> on the two PESs is ascribed to the different structures of the PESs. The reaction mainly proceeds through direct

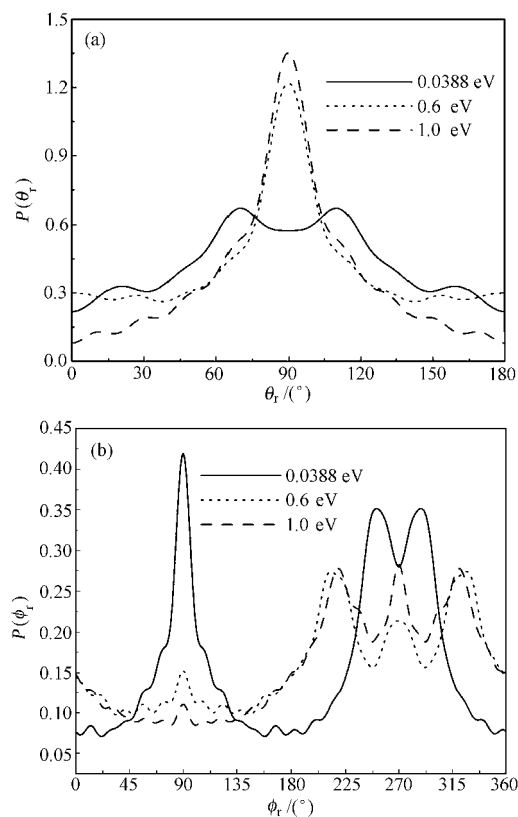


Fig.2 The calculated angular distributions of  $P(\theta_r)$  and  $P(\phi_r)$  on the  $^3A''$  PES at three collision energies

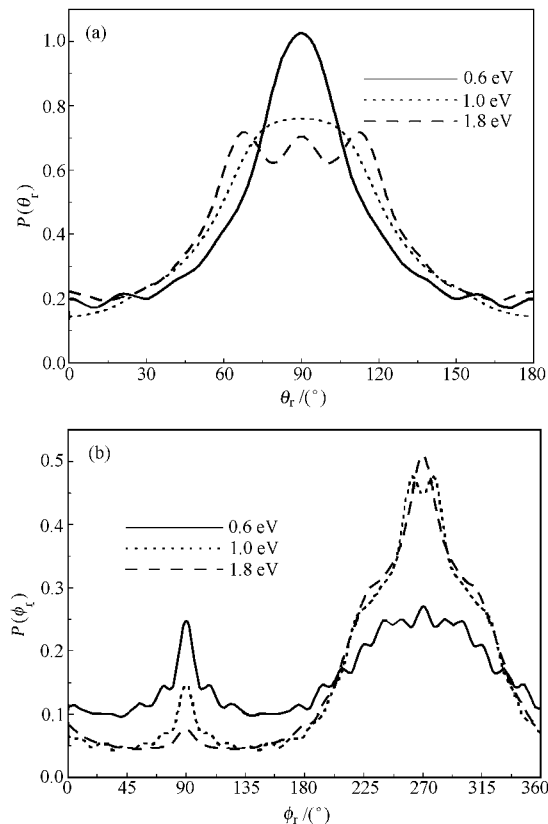


Fig.3 The calculated angular distributions of  $P(\theta_r)$  and  $P(\phi_r)$  on the  $^3A'$  PES at three collision energies

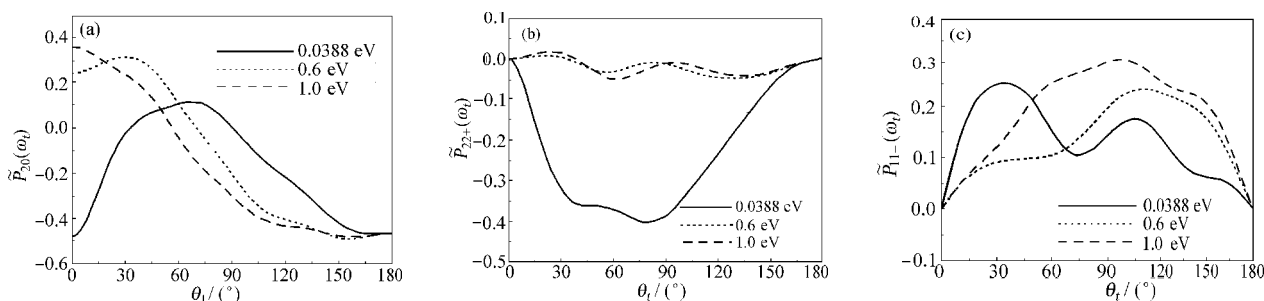


Fig.4 Three renormalized PDDCSs calculated on the  $^3A''$  PES at three collision energies

imum energy path of the  $^3A''$  PES. The maximum impact parameter ( $b_{\text{max}}$ ) decreases from 0.45 nm at 0.0388 eV to 0.26 nm at 1.0 eV, while there exists an energy barrier of 0.3 eV on the  $^3A'$  PES. The parameter  $b_{\text{max}}$  increases from 0.20 nm at 0.6 eV to 0.24 nm at 1.8 eV. For the reaction without barrier, when the collision energy increases, the system rapidly proceeds from the reagents to products and can remain the initial direction "memory". As a result, the product molecule is strongly aligned. However, for the reaction with barrier, the reaction rapidly strides over the energy barrier when the  $E_T$  increases, there is not enough time for the molecule to rotate towards the preferred alignment direction. As a result, the product rotational angular momentum is weakly aligned at high collision energy. In addition, the  $^3A''$  and  $^3A'$  PESs are the attractive and repulsive ones, respectively. Thus, the distributions of  $P(\theta)$  and  $P(\phi)$  on repulsive PES  $^3A'$  are broader than those on attractive  $^3A''$  [21-25].

The renormalized PDDCSs describe the  $\mathbf{k}-\mathbf{k}'-\mathbf{j}'$  correlation. The PDDCSs on the  $^3A''$  PES are shown in Fig.4. The angular distributions of  $\tilde{P}_{20}(\omega_t)$  are drawn in Fig.4(a). The  $\tilde{P}_{20}(\omega_t)$  is related to the expected value  $\langle P_2(\cos\theta_t) \rangle$ . It can be seen from the distributions of  $\tilde{P}_{20}(\omega_t)$  that the  $\mathbf{j}'$  is preferentially polarized along the direction perpendicular to  $\mathbf{k}$  at  $\theta_t=180^\circ$  for the three collision energies.

The angular distributions of  $\tilde{P}_{kqz}(\omega_t)$  with  $q \neq 0$  are depicted in Fig.4(b) and Fig.4(c). The collision energy has a considerable

influence on the angular distributions. All  $\tilde{P}_{kqz}(\omega_t)$  with  $q \neq 0$  are equal to zero at  $\theta_t=0^\circ$  and  $180^\circ$ . The  $\tilde{P}_{22+}(\omega_t)$  and  $\tilde{P}_{11-}(\omega_t)$  are relative to  $\langle \sin^2\theta_t \cos 2\phi_t \rangle$  and  $\langle \sin\theta_t \sin\phi_t \rangle$ , respectively. The values of  $\tilde{P}_{22+}(\omega_t)$  are negative at all scattering angles when  $E_T=0.0388$  eV, as shown in Fig.4(b), which indicates that the product is preferentially aligned along the y-axis. However, when  $E_T=0.6$  and 1.0 eV, the values of  $\tilde{P}_{22+}(\omega_t)$  is almost equal to zero, reflecting that no marked preference of product alignment along y-axis or x-axis, which is consistent with the broad distribution of  $P(\phi_t)$  shown in Fig.2(b). The  $\tilde{P}_{11-}(\omega_t)$  describes the orientation of the product angular momentum  $\mathbf{j}'$  along the y-axis. The  $\mathbf{j}'$  is oriented along the negative direction of y-axis when the value of  $\tilde{P}_{11-}(\omega_t)$  is positive, and along the positive direction of y-axis when the value of  $\tilde{P}_{11-}(\omega_t)$  is negative. It can be seen from Fig.4 (c) that the  $\mathbf{j}'$  is preferentially oriented along the negative direction of y-axis at all scattering angles for three collision energies, which are essentially consistent with the distributions of  $P(\phi_t)$  shown in Fig.2(b).

Fig.5 shows the PDDCSs of the product  $\text{N}_2$  on the  $^3A'$  PES. The distributions of  $\tilde{P}_{20}(\omega_t)$  show that the rotational angular momentum  $\mathbf{j}'$  of the backward scattered products are more preferentially polarized along the direction perpendicular to  $\mathbf{k}$ . The distribution of  $\tilde{P}_{22+}(\omega_t)$  shows that the  $\mathbf{j}'$  is preferentially aligned along the y-axis at all scattering angles. It can be seen from the distributions of  $\tilde{P}_{11-}(\omega_t)$  that when  $E_T=0.6$  eV the  $\mathbf{j}'$  is slightly oriented along the positive direction of y-axis when  $\theta_t < 90^\circ$  and along the negative direction of y-axis when  $\theta_t > 90^\circ$ . The  $\mathbf{j}'$  is

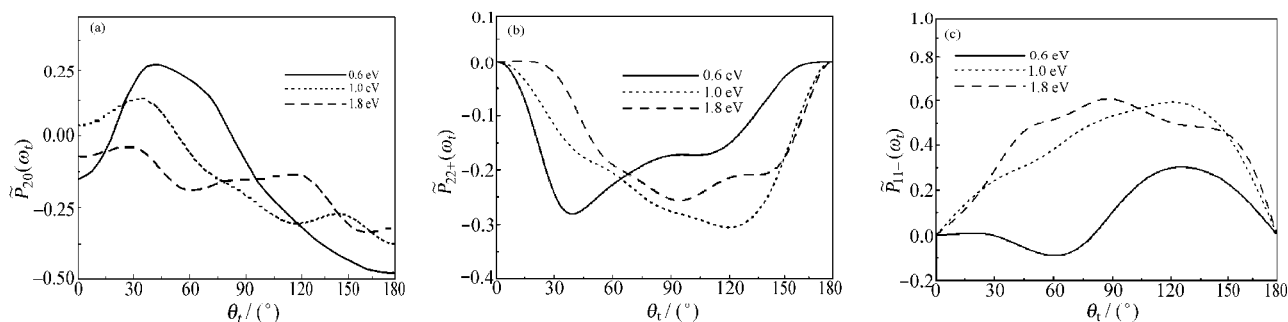


Fig.5 Three renormalized PDDCSs calculated on the  $^3A'$  PES at three collision energies

preferentially oriented along the negative direction of y-axis at all scattering angles when  $E_T=1.0$  and  $1.8$  eV, which is consistent with the distribution of  $P(\phi)$  shown in Fig.3 (b).

### 3 Conclusions

The stereodynamics of reaction  $N(^4S)+NO(X^2II)\rightarrow N_2(X^3\Sigma_g^-)+O(^3P)$  have been studied. The QCT calculated results indicate that the reactions occurred on the  $^3A''$  and  $^3A'$  PESs exhibit different characters and trends for different collision energies. For the reaction occurred on the  $^3A''$  PES, when the collision energy increases, the product rotational angular momentum vector  $\mathbf{j}'$  tends to be aligned along the direction perpendicular to the reagent relative velocity  $\mathbf{k}$  and the reaction is preferentially dominated by out-of-plane mechanism. And the reaction on the  $^3A'$  PES shows that the  $\mathbf{j}'$  is less preferentially aligned along the direction perpendicular to  $\mathbf{k}$  for high collision energy, and the reaction is dominated by in-plane mechanism. All these differences can be ascribed to different constructions of two PESs.

### References

- Siskind, D. E.; Rusch, D. W. *J. Geophys. Res.*, **1992**, **97**: 3209
- Wennberg, P. O.; Anderson, J. G.; Weisenstein, D. K. *J. Geophys. Res.*, **1994**, **99**: 18839
- Warneck, P.; Chemistry of the national atmosphere. San Diego: Academic Press, 1998: Chap. 3
- Marson, G. *Chem. Soc. Rev.*, **1996**, **25**: 33
- Gilibert, M.; Aguililar, A.; González, M.; Mota, F.; Sayós, R. *J. Chem. Phys.*, **1992**, **97**: 5542
- Gilibert, M.; Aguililar, A.; González, M.; Mota, F.; Sayós, R. *J. Chem. Phys.*, **1993**, **99**: 1719
- Duff, J. W.; Sharma, R. D. *Chem. Phys. Lett.*, **1997**, **265**: 404
- Gamallo, P.; González, M.; Sayós, R. *J. Chem. Phys.*, **2003**, **118**: 10602
- Gamallo, P.; González, M.; Sayós, R. *J. Chem. Phys.*, **2003**, **119**: 2545
- Dubrin, J.; Mackay, C.; Wolfgang, R. *J. Chem. Phys.*, **1966**, **44**: 2208
- Iwata, R.; Ferrieri, A.; Wolf, A. P. *J. Phys. Chem.*, **1986**, **90**: 6722
- Kim, S. K.; Herschbach, D. R. *Faraday Discussions. Chem. Soc.*, **1987**, **84**: 159
- Case, D. E.; McClelland, G. M.; Heschbach, D. R. *Mol. Phys.*, **1978**, **35**: 541
- Miranda, M. P.; Clary, D. C. *J. Chem. Phys.*, **1997**, **106**: 4509
- Aoiz, F. J.; Herrero, V. J.; Saez-Rabanos, V. *J. Chem. Phys.*, **1992**, **97**: 7423
- Loesch, H. *J. Phys. Chem. A*, **1997**, **101**: 7461
- Brouard, M.; Gatenby, S. D.; Joseph, D. M.; Vallance, C. *J. Chem. Phys.*, **2000**, **113**: 3162
- Shafer-Ray, N. E.; Orr-Ewing, A. J.; Zare, R. N. *J. Phys. Chem.*, **1995**, **99**: 7591
- Han, K. L.; He, G. Z.; Lou, N. Q. *J. Chem. Phys.*, **1996**, **105**: 8699
- Wang, M. L.; Han, K. L.; He, G. Z. *J. Chem. Phys.*, **1998**, **109**: 5446
- Chen, M. D.; Wang, M. L.; Han, K. L.; Ding, S. L. *Chem. Phys. Lett.*, **1999**, **301**: 303
- Aoiz, F. J.; Bañares, L.; Castillo, J. F.; Martínez-Haya, B.; Marcelo, P. D. M. *J. Chem. Phys.*, **2001**, **114**: 8328
- Chen, M. D.; Han, K. L.; Lou, N. Q. *Chem. Phys. Lett.*, **2002**, **357**: 483
- Chen, M. D.; Han, K. L.; Lou, N. Q. *Chem. Phys.*, **2002**, **283**: 463
- Chen, M. D.; Han, K. L.; Lou, N. Q. *J. Chem. Phys.*, **2003**, **118**: 4463
- Miquel, I.; Hernando, J.; Sayós, R.; González, M. *J. Chem. Phys.*, **2003**, **119**: 10040
- Ma, J. J.; Cong, S. L. *Chin. J. Chem. Phys.*, **2005**, **18**(2): 319 [马建军, 丛书林. 化学物理学报(*Huaxue Wuli Xuebao*), **2005**, **18**(2): 319]
- Ma, J. J.; Cong, S. L.; Zhang, Z. H.; Wang, Y. Q. *Chin. J. Chem. Phys.*, **2006**, **19**(2): 117 [马建军, 丛书林, 张志红, 王艳秋. 化学物理学报(*Huaxue Wuli Xuebao*), **2006**, **19**(2): 117]
- Truhlar, D. G.; Muckerman, J. T. Atom-molecule collision: A Guide for the experimentalists. New York: Plenum Press, 1979: 505
- Aoiz, F. J.; Banares, L.; Herrero, V. J. *J. Chem. Soc., Faraday Trans.*, **1998**, **94**: 2483
- Aoiz, F. J.; Brouard, M.; Enriquez, P. A. *J. Chem. Phys.*, **1996**, **105**: 4964
- Hertel, I. V.; Stoll, W. *Adv. Atom. Mol. Phys.*, **1978**, **13**: 113
- Miranda, M. P.; Aoiz, F. J.; Bañares, L.; Sáez Rábanos, V. *J. Chem. Phys.*, **1999**, **111**: 5368